

## Nanotherapeutics in cancer therapy: targeted delivery-based diagnosis and treatment of cancers

Hyeun Son<sup>1</sup>, Jisu Kim<sup>1</sup>, Hajin Lee<sup>1</sup>, Yunjin Lee<sup>1</sup>, Hongki Kim<sup>2,3, \*</sup>, and Kyung Kwan Lee<sup>1, \*</sup>

<sup>1</sup>Department of Bio-Chemical Engineering, Chosun University, Gwangju, 61452, Korea

<sup>2</sup>Department of Chemistry, Kongju National University, Gongju, 32588, Korea

<sup>3</sup>Earth Environment Research Center, Kongju National University, Gongju, 32588, Korea

(Received March 16, 2026; Accepted March 26, 2026)

**Abstract:** Nanotherapeutics are reshaping cancer management by enabling targeted delivery that integrates selective tumor localization, controlled activation, and diagnostic feedback within a single platform. This review organizes cancer nanotherapeutics from a delivery-first perspective across the full delivery cascade circulation stability, tumor access and retention, intratumoral penetration, cellular internalization, and intracellular trafficking highlighting why fixed nanoparticle properties rarely satisfy all stages simultaneously. We summarize design strategies that reconcile these trade-offs through multistage and stimuli-responsive transitions triggered by endogenous cues or externally applied energy. The tumor microenvironment (TME) is then framed as both a transport barrier and an actionable target, emphasizing delivery programs that remodel or exploit extracellular matrix constraints, hypoxia/acidosis, vascular abnormalities, immune regulation, and tumor-associated communication pathways, including biomimetic and exosome-inspired carriers. We further discuss targeted delivery enabled theranostics, where imaging functions as a quantitative readout of localization, activation, and response dynamics, thereby guiding treatment timing and adaptation. Finally, we integrate therapeutic modalities chemotherapy delivery, catalytic reactive oxygen species-based therapies, energy-activated phototherapy and ultrasound-enabled approaches, and immunotherapy coupling into a mechanistic “combination logic” that is dictated by delivery barriers and TME vulnerabilities. Collectively, this review provides a unified blueprint for designing nanotherapeutics that couple targeted delivery-based diagnosis and treatment to improve precision and therapeutic efficacy.

**Key words:** cancer treatment, targeted delivery, tumor microenvironment, theranostics, and stimuli-responsive nanoparticles

### Introduction

Cancer therapy continues to be limited by off-target toxicity, insufficient drug exposure at tumor

sites, intratumoral heterogeneity, and therapy-induced resistance. While surgery, radiotherapy, systemic chemotherapy, and immunotherapy have expanded clinical options, durable control remains challenging

★ Corresponding author

Phone : +82-(0)41-850-8490

E-mail : hongkikim@kongju.ac.kr, kylee@chosun.ac.kr

This is an open access article distributed under the terms of the Creative Commons Attribution Non-Commercial License (<http://creativecommons.org/licenses/by-nc/3.0>) which permits unrestricted non-commercial use, distribution, and reproduction in any medium, provided the original work is properly cited.

for many advanced or heterogeneous tumors. A central unmet need is therefore the ability to increase tumor-selective exposure while minimizing systemic burden and enabling adaptive treatment based on real-time assessment of delivery and response.<sup>1-3</sup> Nanotherapeutics have emerged as a practical strategy to address these limitations by re-engineering how therapeutic and diagnostic agents travel through the body and interact with tumors. By packaging drugs and imaging probes into nanoscale carriers, nanotherapeutics can improve solubility, circulation half-life, and biodistribution, and they can co-deliver multiple agents to enable rational combination therapy in a single formulation. Importantly, nanoplatforms can be designed not only to transport payloads, but also to sense and respond to tumor-associated cues, thereby linking delivery to activation and minimizing off-target effects.<sup>4</sup> Importantly, nanomaterials can serve as a unifying scaffold that physically integrates therapeutic payloads with diagnostic reporters, giving rise to theranostic systems capable of simultaneous treatment and real-time monitoring

(Fig. 1)

At the foundation of systemic nanodelivery is tumor accumulation driven by the enhanced permeability and retention (EPR) effect; however, EPR is heterogeneous and rarely guarantees deep, uniform penetration. Successful nanotherapy requires coordinated performance across a delivery cascade stable circulation, tumor access and retention, penetration through physical barriers, cellular internalization, and intracellular trafficking yet these stages impose contradictory physicochemical requirements.<sup>5-7</sup> For example, properties favoring long circulation and accumulation may not favor penetration or uptake, motivating multistage designs in which size, surface charge, or ligand availability changes in situ. Consequently, stimuli-responsive strategies that trigger controlled transitions within tumor regions have become central to delivery-first nanotherapeutic engineering.<sup>8</sup>

The tumor microenvironment (TME) is both a major barrier and an exploitable trigger space. Abnormal vasculature, elevated interstitial pressure, and dense

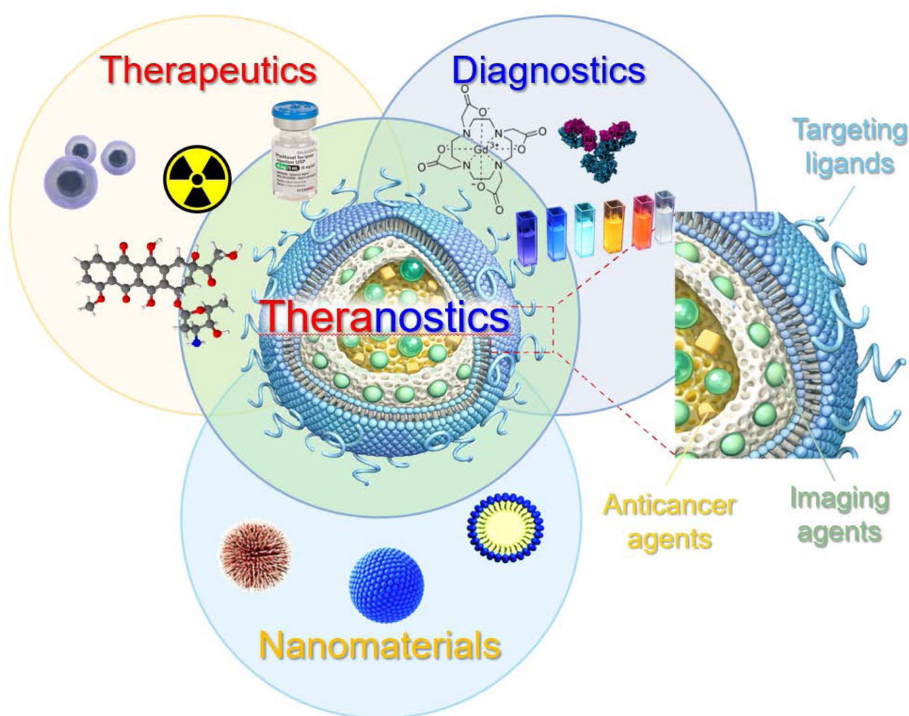


Fig. 1. Concept of theranostics enabled by nanomaterials.

extracellular matrix can restrict transport, while hypoxia and acidosis contribute to metabolic adaptation and therapeutic resistance. At the same time, these features provide endogenous cues for selective activation and targeted release. In parallel, biomimetic delivery systems including cell membrane-functionalized constructs and exosome-inspired carriers offer complementary routes to enhance tumor localization, modulate immune interactions, and improve intracellular delivery pathways.<sup>9,10</sup>

Accordingly, this review focuses on targeted delivery-based diagnosis and treatment as a unified framework for cancer nanotherapeutics. We first summarize core principles of targeted delivery and multistage targeting across tissue-, cell-, and intracellular-level barriers. We then discuss key design parameters that govern delivery performance, followed by TME-targeted delivery strategies that remodel or exploit tumor transport constraints and regulatory niches.<sup>9,11</sup> Next, we highlight delivery-enabled diagnosis and monitoring, emphasizing theranostic imaging as a functional readout of localization, activation, and response. Finally, we integrate major therapeutic modalities into a delivery-guided combination logic that leverages TME vulnerabilities and externally controllable triggers to improve therapeutic precision.

## 2. Core Principles of Targeted Delivery in Cancer Nanotherapeutics

Targeted delivery in cancer nanomedicine is best understood as a sequential delivery cascade rather than a single event: (i) prolonged circulation and tumor access, (ii) extravasation and intratumoral retention, (iii) deep penetration through a heterogeneous TME, and (iv) efficient cellular internalization. Because each step is governed by different biological barriers, “targeting” is typically implemented through passive targeting (EPR-driven accumulation), active targeting (ligand-receptor recognition), and increasingly hierarchical/multistage targeting that dynamically adapts nanoparticle properties in response to tumor-associated stimuli.

### 2.1. Passive targeting: EPR-driven tumor accumulation and its limits

Passive targeting relies on the enhanced permeability and retention (EPR) effect, which arises from leaky tumor vasculature and inefficient lymphatic drainage. In solid tumors, deficient lymphatic drainage disrupts interstitial fluid transport such that macromolecules and nanoparticles that extravasate into the tumor interstitium can be retained for prolonged periods.<sup>12</sup> In parallel, abnormal neovascularization with enlarged vascular pores promotes nanoparticle extravasation and accumulation, while poor lymphatic drainage further increases retention.<sup>12,13</sup>

However, EPR-mediated delivery is highly sensitive to nanoparticle physicochemical properties (size, shape, surface features/charge) and to tumor pathophysiology.<sup>12-14</sup> For example, very small constructs near the renal filtration threshold exhibit short circulation times, whereas large particles (>200 nm) show poor extravasation; thus, nanoparticles in the ~50–150 nm range are often considered favorable for EPR-mediated tumor targeting.<sup>14</sup> Surface charge is similarly influential: highly cationic particles can be trapped by negatively charged endothelial luminal surfaces, while strongly anionic particles are prone to clearance by the reticuloendothelial system; therefore, near-neutral or slightly negative surfaces are commonly preferred for systemic delivery.

Crucially, the EPR effect is heterogeneous across patients, tumor types, and even within the same tumor over time, leading to widely variable clinical benefit from systemically administered nanomedicines.<sup>15</sup> This variability is linked to differences in tumor vascular density, perfusion status, stromal composition, and other pathophysiological features.<sup>15,16</sup> In addition, even when nanoparticles reach tumors, abnormal vasculature and elevated interstitial fluid pressure can reduce homogeneous distribution, often causing perivascular localization and peripheral accumulation rather than deep penetration.<sup>17,18</sup> These limitations motivate strategies that go beyond passive targeting alone, such as TME-priming and smart delivery systems that exploit tumor-local cues for improved penetration and activation.<sup>16-18</sup>

## 2.2. Active targeting: ligand receptor recognition for selective cellular uptake

Active targeting seeks to increase selectivity at the cellular or vascular level by decorating nanocarriers with targeting moieties (e.g., antibodies, proteins, peptides, aptamers) that bind receptors overexpressed on tumor cells or tumor-associated endothelium. In practice, active targeting most often acts after the carrier has already accumulated in the tumor region (frequently via EPR), and its main advantage is improved cellular binding and internalization rather than guaranteed tumor homing from blood.

A broad set of ligands has been employed. Protein ligands such as transferrin and epidermal growth factor have been used to guide nanoparticles to corresponding overexpressed receptors (e.g., TfR, EGFR), and cell-adhesion proteins (cadherins, integrins, selectins) provide additional routes for targeting cancer cell membranes or tumor vasculature.<sup>19</sup> Among peptide ligands, RGD-based peptides are widely used because they bind integrin  $\alpha\beta_3$ , which is enriched in tumor cells and supporting vasculature; RGD decoration has been applied across multiple payload classes (siRNA, chemotherapy, photothermal and photodynamic agents) to reduce off-target toxicity while suppressing tumor growth and angiogenesis.<sup>20</sup>

For prostate cancer, prostate-specific membrane antigen (PSMA) is a representative and clinically relevant active-targeting axis. PSMA is overexpressed on malignant prostate cells, and PSMA-functionalized theranostic nanoparticles have shown improved selectivity and intracellular drug accumulation compared with non-targeted systems.<sup>21</sup> Mechanistically, PSMA behaves like a cell surface receptor with a large extracellular domain enabling antibody access, and PSMA-antibody complexes can be rapidly internalized features that support PSMA-targeted nanoparticle delivery.<sup>21,22</sup>

A key nuance is that “more ligand” is not always better. In PSMA-targeted systems, increased antibody density on nanoparticle surfaces does not necessarily improve PSMA-specific targeting; instead, targeting performance reflects an optimized combination of surface chemistry, PEGylation, and ligand density.<sup>23</sup>

More generally, circulating nanoparticles are prone to opsonization and formation of a protein corona, which can mask ligands and accelerate clearance; PEGylation and related stealth coatings are frequently used to reduce opsonin adsorption and prolong circulation.<sup>24</sup> These realities mean that active targeting must be engineered as part of an integrated delivery program rather than as a standalone “address label.”

## 2.3. Hierarchical and multistage targeting: resolving trade-offs across the delivery cascade

Because the requirements for circulation, tumor accumulation, penetration, cellular uptake, and organelle localization can be paradoxical, it is increasingly recognized as unrealistic for a nanocarrier with fixed size/charge/surface modifications to perform optimally at every step.<sup>25</sup> For example, relatively larger particles (tens to  $\sim 200$  nm) support prolonged circulation and EPR-mediated accumulation, whereas smaller particles ( $\sim 10$ - $20$  nm) better enable deep tumor penetration; similarly, neutral/slightly anionic surfaces favor long circulation, but cationic surfaces enhance uptake via electrostatic interactions and can support endosomal escape.<sup>14,26</sup> Targeting ligands also pose a dilemma: ligands are useful for accurate tumor cell/organelle delivery, but can engage nonspecific serum interactions and immune recognition during circulation, compromising targeting efficiency.<sup>23,27</sup>

To reconcile these constraints, modern cancer nanotherapeutics increasingly employ stimuli-responsive multistage targeting, in which size reduction, charge conversion, and ligand exposure are triggered selectively within tumors by endogenous or exogenous stimuli.<sup>28</sup> A representative approach is ligand shielding and re-exposure: ligands can be buried under a PEG corona during circulation and then exposed at tumor sites via tumor-local triggers (e.g., acidity-triggered de-PEGylation), improving both circulation half-life and tumor cell internalization.<sup>29</sup> Conceptually, such strategies enable sequential targeting across tumor tissue, tumor cells, and organelles by using local cues (pH, redox gradients, enzymes, ATP, hypoxia) or external stimuli (ultrasound, light, magnetic fields) to reconfigure nanoparticle behavior at the right place

and time.<sup>30</sup>

Size-shrinkable designs exemplify the multistage principle. Enzyme-triggered size reduction can be achieved using MMP-2/9 or hyaluronidase (HAase), which are enriched in the TME, to convert ~100 nm constructs into ~10 nm components that diffuse more effectively within tumor interstitium.<sup>31</sup> Beyond penetration, charge-reversible systems can also implement two-step activation remaining negatively charged for circulation, then switching to positive charge in the tumor/endolysosomal environment to favor mitochondrial targeting and metabolic disruption.<sup>32</sup>

Taken together, these principles suggest that the most effective “targeted delivery” architectures are not defined solely by a single targeting ligand or a single mechanism, but by how well a platform coordinates multiple delivery tasks: circulation, accumulation, penetration, uptake, and intracellular trafficking through programmable or tumor-triggered transitions. This delivery first perspective provides a practical foundation for the subsequent sections on material design variables, TME-targeted strategies, and theranostic integration.

### 3. Design Parameters for Target Delivery- Optimized Nanotherapeutics

Rational nanotherapeutic design begins with a simple premise: delivery performance is an emergent outcome of (i) the carrier platform, (ii) its physicochemical properties in blood, (iii) surface/interface engineering at the bionano boundary, and (iv) the payload loading/release mechanism. Because tumors impose stage-specific and often contradictory requirements, modern designs increasingly use programmable transitions (size/charge/ligand exposure changes) to maintain circulation stability while activating penetration and uptake only after reaching tumor sites.

#### 3.1. Platform selection: material class and architecture

Carrier choice sets the “design space” for achievable loading capacity, stability, imaging compatibility, and stimulus responsiveness. Broadly, platforms include

organic (lipid/polymer), inorganic (metals/metal oxides, silica, carbon), and hybrid systems.

Hybrid nanocarriers are increasingly used to combine complementary functions e.g., inorganic components for imaging/photothermal conversion with polymer/lipid shells for biocompatibility and controlled release. Inorganic metallic nanostructures (e.g., Au, Ag) provide size-tunable physicochemical properties that support photothermal therapy and can be integrated with targeting and imaging agents; hybridization via versatile surface chemistry enables multi-functional architectures.<sup>33</sup>

Alongside synthetic carriers, biomimetic systems (cell membrane-coated nanoparticles) and exosome-based delivery offer a distinct route to tumor targeting and intracellular transport. Exosomes can carry small molecules and nucleic acids (siRNA/miRNA), and recipient cells can internalize exosomes via multiple endocytosis pathways, lowering the energy barrier for uptake in some contexts.<sup>34</sup> Because exosomes are naturally derived, they are often described as having superior biocompatibility and reduced immunogenicity relative to many synthetic nanocarriers, with intrinsic immune tolerance noted as a potential safety advantage.<sup>35</sup>

#### 3.2. Physicochemical properties: size, shape, charge, and stability

After platform choice, size and surface charge are the most influential levers for systemic delivery because they govern circulation half-life, renal clearance, extravasation, and cellular uptake. Reviews commonly note that maintaining particle size in the tens-to-low hundreds of nanometers can improve circulation and reduce renal filtration, while sizes around 50–200 nm are often considered favorable for prolonged circulation and tumor accumulation.<sup>36</sup> However, even with favorable sizes, multiple tumor-side barriers can hinder delivery and penetration.<sup>37</sup>

Surface charge introduces a similar trade-off. Neutral or slightly negative particles are often associated with longer circulation and improved accumulation, while cationic surfaces can accelerate clearance yet enhance cellular uptake through electrostatic interactions.<sup>38</sup>

These paradoxical requirements underpin why

“fixed-property” nanoparticles often fail to optimize all delivery stages.<sup>36-38</sup>

A practical and sometimes underappreciated parameter is colloidal stability under physiological protein conditions. Nanoparticles entering the body are prone to opsonization and formation of a protein corona, which can alter biodistribution, mask targeting ligands, and promote clearance.<sup>39</sup> Consequently, design should explicitly consider how surface chemistry evolves in serum rather than assuming an “as-synthesized” surface.

### 3.3. Surface/interface engineering

#### 3.3.1. Stealth coatings and immune clearance control

To reduce opsonin adsorption and reticuloendothelial clearance, hydrophilic stealth coatings most commonly PEGylation are widely used. PEGylation is frequently described as a strategy to reduce opsonin adsorption and mitigate protein-corona-driven clearance.<sup>2,23</sup>

#### 3.3.2. Targeting ligands

Active targeting via antibodies/peptides/small molecules improves binding/internalization at tumor sites, but ligand choice and density must be optimized. Importantly, increased antibody density does not necessarily increase target specificity; in PSMA-targeted iron oxide nanoparticles, improved PSMA targeting depended on an optimized combination of

surface chemistry, PEGylation, and antibody density rather than antibody density alone.<sup>22,23</sup> This is consistent with the general notion that ligands can drive nonspecific serum interactions and immune recognition during circulation, compromising targeting efficiency unless properly shielded.

#### 3.3.3. Stimuli-triggered ligand exposure

A widely used solution is “shield in blood, expose in tumor”. One common strategy is to bury targeting moieties under a PEG corona during circulation and then detach PEG in tumors to expose ligands and enhance internalization.<sup>29</sup> Acid-sensitive linkers can enable pH-triggered PEG detachment, while tumor-overexpressed enzymes such as MMP2 can cleave PEG linkers to expose cell-penetrating peptides or RGD motifs specifically in the tumor microenvironment.<sup>40</sup>

### 3.4. Payload loading and release logic

Delivery outcomes also depend on whether the payload is encapsulated (diffusion-controlled release), conjugated (cleavable linkers), or co-assembled (carrier-free or coordination-driven assemblies). Hybrid and prodrug designs can couple drug release with microenvironmental activation and therapeutic amplification.

A representative example is a pH-, reduction-, and near infrared (NIR) light-sensitive nanodrug system constructed from doxorubicin and a platinum (IV)

Table 1. Design knobs vs. delivery stage for cancer nanotherapeutics

	Circulation	Tumor accumulation	Intratumoral penetration	trafficking & release
Size	Larger (~50–150 nm) often prolongs circulation; too small (<10 nm) risks rapid renal clearance	Intermediate size supports EPR-mediated accumulation	Smaller (~10–30 nm) penetrates deeper	Disassembly into smaller components improves cytosolic/organellar access
Shape	Spherical often stable; anisotropic shapes may alter clearance but complicate reproducibility	Shape affects margination/extravasation	High aspect ratio may hinder diffusion through dense ECM	Shape affects endosomal escape and intracellular routing
Surface charge	Near-neutral/slightly negative reduces opsonization and prolongs circulation	Strongly charged surfaces increase nonspecific interactions/clearance	Mildly positive may increase ECM sticking	Charge-switching (neutral/negative → positive) supports endosomal escape
Ligand type & density	Too high density can increase serum interactions	Improves binding in tumor region	Early/strong binding can trap particles perivascularly	Can support organelle targeting when paired with trafficking motifs
Mechanical rigidity	Softer particles may evade phagocytosis	Deformability can improve microvascular transport	Deformable carriers may traverse tight interstitium better	Influences endosomal escape/persistence
Biomimetic coating	Improves immune evasion; can prolong circulation	May enhance homotypic targeting/retention	May aid stromal navigation depending on surface proteins	Facilitates intracellular delivery with reduced immunogenicity
Stimuli-responsive switching	Stable “off” state protects payload in blood	Tumor-local “on” state increases functional dose	Size shrinkage + ECM-responsive shedding increases diffusion	Intracellular triggers synchronize release at target location

prodrug, with  $\text{Cu}^{2+}$ -driven coordination assembly and a polydopamine (PDA) coating. In tumor cells, elevated glutathione (GSH) reduces  $\text{Pt(IV)}$  and  $\text{Cu}^{2+}$  to active  $\text{Pt(II)}$  and  $\text{Cu}^+$ , inducing drug release, GSH depletion, and nanoparticle disassembly; meanwhile, PDA provides photothermal conversion for mild photothermal therapy (PTT), illustrating how intracellular redox activation + external NIR control can be integrated into a single formulation.<sup>41</sup>

### 3.5. Stimuli-responsive modules: programmable transitions for multistage delivery

Because each delivery stage favors different properties, stimuli-responsive design has become a central engineering principle. It is explicitly noted that it is unrealistic to expect a nanocarrier with fixed size/charge/surface modifications to satisfy tumor tissue, cell, and organelle targeting simultaneously, and that endogenous (pH, redox, enzyme/ATP) or exogenous (temperature, magnetic fields, ultrasound, light) stimuli can be used to trigger size reduction, charge conversion, and ligand exposure.<sup>28,42</sup>

#### 3.5.1. Endogenous triggers

Enzyme-responsive systems can exploit tumor-associated proteases (e.g., MMPs, cathepsins, hyaluronidase) to degrade carriers and improve stromal penetration, while redox-responsive systems use elevated intracellular glutathione to cleave disulfide bonds for selective intracellular release (Lambuk *et al.*, 2026).<sup>31</sup>

#### 3.5.2. Exogenous triggers

Thermo-responsive systems can be activated by localized hyperthermia (e.g., focused ultrasound or magnetic nanoparticle heating), and NIR-light responsive systems can enable on-demand release or photothermal/photodynamic co-therapy, albeit with tissue penetration limits.<sup>43</sup>

#### 3.5.3. Size shrinkage and charge conversion.

Multistage frameworks often aim for “large in blood, small in tumor” behavior; one example described is a clustered nanoparticle (~100 nm) that shrinks to

~5 nm in acidic tumor extracellular pH, enabling deeper penetration in poorly permeable tumors.<sup>2,44</sup>

Charge-reversible nanomedicines are similarly used to maintain long circulation in a neutral/negative state and then convert to cationic surfaces in tumors to enhance transcytosis, uptake, and even mitochondrial targeting.<sup>45</sup> Collectively, these parameters impose stage-specific and often opposing requirements across the delivery cascade. A practical summary of how key design ‘knobs’ influence each delivery stage and where major trade-offs arise is provided in *Table 1*.

## 4. Tumor Microenvironment-targeted Delivery Strategies

The TME is not only the dominant barrier that limits homogeneous intratumoral distribution of nanotherapeutics, but also a programmable target space rich in biochemical and biophysical cues that can be exploited for selective activation. Recent frameworks therefore treat TME-targeting as a delivery “amplifier,” where extracellular matrix (ECM) remodeling, hypoxia/acidosis adaptation, vascular modulation, immune reprogramming, stromal control, and exosome/extracellular vesicle (EV) engineering are integrated to improve both delivery efficiency and therapeutic specificity.<sup>46</sup>

These interconnected TME-modulating strategies are conceptually illustrated in *Fig. 2*.

### 4.1. ECM as a transport barrier and a delivery target

Dense and aberrantly organized ECM is a major cause of poor penetration and heterogeneous drug exposure. In many solid tumors, the ECM exhibits excessive deposition, abnormal composition, increased stiffness, and disordered architecture, collectively impeding diffusion and penetration of therapeutics.<sup>47,48</sup> Accordingly, ECM-targeted delivery often pursues either (i) direct degradation/normalization of ECM components or (ii) transient physical opening of transport pathways.

#### 4.1.1. Enzymatic ECM remodeling

Collagenase-mediated degradation of fibrillar collagen

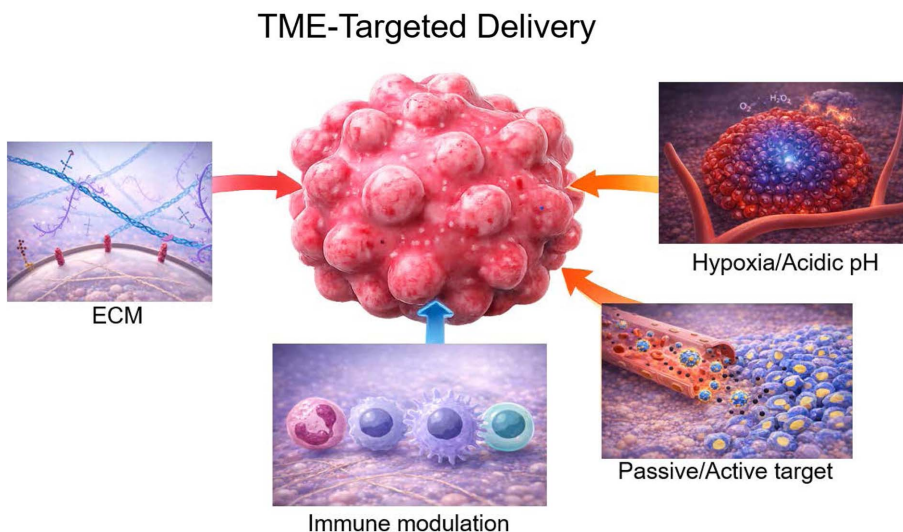


Fig. 2. TME-targeted delivery strategies for enhancing nanotherapeutic efficacy.

can reduce stiffness and improve penetration, while hyaluronidase-driven breakdown of hyaluronic acid can lower interstitial fluid pressure (IFP) and facilitate deeper diffusion of nanocarriers.<sup>49</sup> These approaches can be implemented by enzyme-functionalized nanoparticles, macromolecules, or engineered cells capable of local enzyme release to increase intratumoral distribution and efficacy.<sup>50</sup>

#### 4.1.2. Physical/energy-assisted ECM priming.

Photoactivatable and externally triggered strategies aim to generate localized heat, ultrasound-induced cavitation, or reactive oxygen species (ROS) to degrade ECM and transiently open diffusion pathways, thereby weakening ECM barriers prior to or during therapeutic delivery.<sup>51,52</sup>

### 4.2. Targeting hypoxia and acidosis as endogenous triggers for selective activation

Hypoxia and acidosis are hallmark features of many solid tumors and are tightly coupled to metabolic reprogramming and therapeutic resistance. Oxygen imbalance generates spatially distinct normoxic, hypoxic, and necrotic regions; in hypoxic regions, tumor cells reorganize metabolism to preserve energy production and survival.<sup>53</sup> A central molecular axis

is stabilization and activation of hypoxia-inducible factors, especially HIF-1 $\alpha$ , which drives glycolysis/angiogenesis programs and supports survival under low oxygen.<sup>54</sup>

#### 4.2.1. Acidosis from glycolytic shift and lactate export

Under hypoxia, tumors shift toward glycolysis with elevated lactate production; excess lactate export contributes to TME acidification, which is associated with increased aggressiveness, immune suppression, and even ECM remodeling.<sup>55</sup>

#### 4.2.2. pH-responsive delivery logic

Because tumor cells thrive in low oxygen and acidic conditions supported by high lactic acid output, pH-responsive nanotherapeutics are often designed to remain stable at physiological pH but become degradable/activatable at tumor pH.<sup>56</sup> In practice, this can manifest as acidity-triggered carrier disassembly, “pop-up” ligand exposure (i.e., shielding during circulation and activation in tumors), or pH-accelerated payload release that sharpens on-target selectivity.

#### 4.2.3. Hypoxia-triggered multistage transitions

Hypoxia can also be used as a stimulus for charge

conversion and size reduction to improve penetration and internalization; for example, hypoxia-responsive systems have been reported to reverse charge and reduce size under hypoxic conditions, aligning with multistage delivery needs.<sup>57</sup>

#### 4.2.4. Theranostic coupling

In prostate cancer, hypoxia-driven glycolysis and HIF-1 $\alpha$  signaling are highlighted as druggable axes where theranostic nanoparticles can combine imaging and therapy while targeting HIF-1 $\alpha$  and downstream metabolic pathways.<sup>58</sup>

#### 4.3. Tumor vasculature and neovascular niches: access, retention, and spatial control

Abnormal tumor vasculature contributes to uneven perfusion and delivery heterogeneity, but also offers targetable endothelial/pericyte-associated markers. A TME-centered view explicitly includes “preventing neovascularization” as a delivery-relevant strategy because vascular normalization or inhibition can reshape perfusion, permeability, and interstitial transport.<sup>59</sup>

From a design standpoint, vascular targeting is most effective when integrated with downstream penetration and cellular uptake modules otherwise, nanoparticles may remain perivascular. Thus, vasculature-focused targeting is commonly paired with ECM priming and stimulus-responsive activation to enhance deep distribution.

#### 4.4. Immune microenvironment targeting.

The immune compartment is a decisive regulator of tumor progression and also a powerful delivery handle. In particular, tumor-associated macrophages (TAMs) are abundant in many tumors and often exhibit an M2-like, pro-tumor phenotype that supports angiogenesis, immune evasion, and matrix remodeling.<sup>60</sup> This has motivated delivery strategies that either (i) directly target TAMs to deplete or reprogram them, or (ii) exploit macrophage biology to enhance delivery.

##### 4.4.1. TAM reprogramming logic.

Reprogramming TAMs from tumor-promoting M2-like states toward tumoricidal M1-like states is

widely pursued because it can disrupt tumor-supporting TME functions and improve anti-tumor immunity.<sup>61</sup>

##### 4.4.2. Macrophage membrane-coated nanoparticles

Biomimetic coating with macrophage membrane provides a multifunctional approach: it can reduce immune-system uptake and premature leakage while improving interactions with cancer cells via membrane proteins, extending circulation time and enhancing targeted delivery.<sup>34,62</sup> These platforms also retain inherent proteins/receptors that support tumor-targeted interactions and immune modulation, contributing to immune evasion and improved tumor targeting.

##### 4.4.3. Checkpoint and axis targeting via biomimicry

Beyond passive camouflage, macrophage-membrane designs can be engineered to target immune checkpoints or macrophage recruitment pathways to overcome immunosuppression while simultaneously delivering therapeutic payloads.<sup>63</sup>

##### 4.5. Stromal fibroblasts and desmoplasia

Stromal fibroblasts can impose transport and signaling resistance. Fibroblasts have been reported to obstruct medication penetration, and fibroblastic cells can enhance resistance to cytotoxic agents through soluble factors and direct interactions with cancer cells.<sup>64</sup> In highly desmoplastic tumors, excessive ECM deposition and fibroblast activation create a dense stromal response that physically limits penetration and can contribute to local immunosuppression by restricting immune-cell infiltration.<sup>65</sup>

This motivates strategies such as stromal priming (ECM/interstitial fluid pressure modulation), fibroblast-targeted delivery, and combination approaches that address both stromal barriers and tumor cell killing. At the conceptual level, “CAF depletion” is frequently discussed as one route to disrupt stromal tumor interactions and combat progression.<sup>66</sup>

##### 4.6. Exosomes and EV pathways

Exosomes are increasingly positioned as both TME communication mediators and delivery carriers. In TME schematics, exosomes are described as major

drivers of tumor growth/modification and as key mediators of autocrine and paracrine communication, including conversion of neighboring normal cells toward tumor-associated phenotypes.<sup>3,67</sup>

#### 4.6.1. Mechanistic advantages for delivery

Exosome-mediated delivery can transport diverse payloads (small molecules, siRNA/miRNA), and exosome uptake can be facilitated by lipid-raft interactions that lower the energy barrier for endocytosis, as well as by protein-mediated internalization via clathrin- or caveolin-dependent pathways.<sup>68</sup>

#### 4.6.2. Biocompatibility and immune profile

Because exosomes are naturally derived, they are often described as having superior biocompatibility and reduced immunogenicity compared with many synthetic nanocarriers, exhibiting intrinsic immune tolerance that can offer a safer *in vivo* delivery profile.<sup>69</sup>

## 5. Targeted Delivery-based Diagnosis: Imaging and Monitoring

Targeted delivery and diagnosis are increasingly co-developed as a single design objective in cancer nanotherapeutics. Theranostic nanoparticles are explicitly conceived to integrate diagnostic and therapeutic functions within one platform, enabling real-time tumor imaging alongside site-specific drug delivery to enhance treatment precision and reduce systemic toxicity.<sup>70</sup>

### 5.1. Imaging modalities enabled by nanotherapeutic platforms

Nanotherapeutics support multiple imaging modalities often in the same construct through incorporation of contrast-generating cores, activatable shells, or co-loaded probes.

#### 5.1.1. MRI-centric and switchable contrast designs

Mn-based nanotherapeutics are frequently used to realize tumor-activated magnetic resonance imaging (MRI), because Mn-containing components can be engineered to “turn on” in acidic or intracellular

environments. For example, MnO<sub>2</sub>-containing systems can decompose to Mn<sup>2+</sup> in acidic tumor regions, improving MRI signals and enabling detection of acidic microenvironments.<sup>71</sup> Similarly, core-shell constructs have been described to transform from T<sub>2</sub> (dark) contrast outside cells to T<sub>1</sub> (bright) contrast within cells, supporting spatially resolved readout of intracellular delivery.<sup>72</sup> Dual-modal radionuclide MRI strategies are also used; for instance, manganese oxide-based systems labeled with radioisotopes have been employed for single-photon emission computed tomography-MRI dual imaging.<sup>73</sup>

#### 5.1.2. CT/NIR and multimodal image-guided platforms

Biomimetic and inorganic hybrid nanotherapeutics frequently integrate computed tomography (CT) and optical/NIR modalities to combine anatomical localization with functional readouts. In macrophage membrane functionalized nanotherapeutics, iron-based components were highlighted for efficient MRI, enabling monitoring of biodistribution and therapeutic progress.<sup>74</sup> In the same context, hollow bismuth selenide nanoparticles were described as effective for CT imaging (high resolution and 3D visualization) and infrared thermal imaging, enabling multi-angle treatment guidance.<sup>75</sup> More advanced designs also incorporate Raman reporters. For instance, a hybrid system has been reported to enable multimodal image-guided therapy using second near-infrared window (NIR-II) photoacoustic (PA) and fluorescence (FL) imaging, while also offering a surface-enhanced Raman scattering reporter for additional molecular readouts.<sup>76</sup>

### 5.2. Activatable imaging

Because tumor delivery is heterogeneous, activatable (turn-on) imaging is particularly valuable: it can reduce background signals and report when/where a nanotherapeutic reaches an intended microenvironmental niche. Acid-activated MRI is a representative example, where MnO<sub>2</sub> decomposition in acidic tumor regions generates Mn<sup>2+</sup> and enhances imaging signals thereby functioning as both a contrast mechanism and a proxy for tumor-local activation.<sup>77</sup>

Hypoxia-activated imaging provides another powerful delivery readout. A molecular probe system was described to generate strong, turn-on NIR-II FL and photoacoustic signals under hypoxic conditions, enabling *in situ* illumination of hypoxic tumors and offering image guidance for subsequent therapy.<sup>78</sup> Notably, in this type of design, the imaging channel is mechanically coupled to therapy, allowing a single platform to (i) identify the resistant niche, (ii) confirm local activation, and (iii) guide therapeutic irradiation or sequencing.<sup>79</sup>

From a manuscript-organization perspective, it is useful to present these systems as “diagnosis of delivery” rather than “diagnosis of cancer” alone: imaging signals can be interpreted as evidence of (a) tumor localization, (b) microenvironmental activation, and (c) longitudinal treatment response.

### 5.3. Biomarker-linked diagnosis and longitudinal monitoring

Beyond imaging contrast, targeted nanotherapeutics can be designed to report molecular biomarkers relevant to diagnosis or response. For instance, a macrophage membrane camouflaged system was described where a fluorescent signal enabled identification of a miRNA-21 biomarker for diagnosis, while the therapeutic module induced mitochondrial dysfunction and apoptosis.<sup>80</sup>

This illustrates a broader direction: combining targeted delivery with signal generation that directly corresponds to tumor-associated biomarkers, thereby linking diagnosis with mechanistic therapy.

Longitudinal monitoring is particularly important in anatomically constrained or barrier-limited sites. In glaucoma-associated ocular cancers, conventional imaging modalities were described as limited by insufficient resolution/sensitivity and difficulty visualizing functional changes; this diagnostic gap was positioned as an opportunity for nanotechnology-enhanced imaging.<sup>43</sup> In this context, nanoparticle-based imaging agents (including FL dyes, radioactive isotopes, and MRI contrast agents) were described as enabling early detection by selectively accumulating in affected ocular tissues, with multimodal combinations improving detection accuracy through complementary optical and anatomical information.<sup>81</sup> The same review also highlighted nanosensor concepts for continuous monitoring of intraocular pressure, emphasizing real-time disease tracking rather than snapshot assessments.<sup>82</sup> To translate diagnostic readouts into actionable treatment decisions, major TME hallmarks can be mapped to delivery strategies, imaging signals that report localization/activation, and therapeutic modules that exploit the same vulnerability; this delivery-guided theranostic decision matrix is summarized in *Table 2*.

*Table 2.* TME vulnerability-guided theranostic treatment matrix

TME feature	Delivery strategy	Imaging readout	Therapy modul	Expected synergy
Dense ECM	ECM-priming (enzyme-assisted degradation, matrix-relaxing modules, sheddable coatings)	Penetration mapping via FL/PA signal spread; pre/post-priming distribution	Chemotherapy + penetration enhancers; delayed release after diffusion	Improves intratumoral uniformity; reduces perivascular trapping
Hypoxia	Hypoxia-activated switches; O <sub>2</sub> -generating catalysts	Hypoxia-activatable FL/PA “turn-on” signals; oxygenation-sensitive contrast	PDT support via O <sub>2</sub> generation; SDT/ROS modules for hypoxic niches	Converts resistant niche into treatable zone; imaging confirms activation
Acidosis	pH-triggered de-shielding, charge conversion, disassembly	pH-activatable probes; “turn-on” contrast in acidic regions	pH-triggered drug release; PTT-assisted uptake/release	Confines activation to acidic tumor compartments
High intracellular GSH	Redox-cleavable linkers; GSH depletion; redox-triggered disassembly	Redox-activatable reporters; signal changes upon disassembly	CDT amplification (less ROS quenching); chemo sensitization; ICD promotion	Overcomes redox resistance; boosts ROS-mediated killing
Elevated H <sub>2</sub> O <sub>2</sub> / oxidative chemistry	Fenton/Fenton-like catalysts	Catalysis-linked signals (e.g., MRI “turn-on” via ion release; PA/FL changes)	CDT (-OH generation) ± PTT/SDT co-amplification	Uses endogenous H <sub>2</sub> O <sub>2</sub> to drive local cytotoxic chemistry
Immunosuppressive TAM-rich TME	TAM targeting/reprogramming; macrophage membrane camouflage; immune-evasive coatings	Immune-cell-associated tracking; biodistribution/retention of biomimetic carriers	ICD-inducing chemo/ROS + immune activation (cGAS-STING) ± checkpoint synergy	Improves delivery and remodels immune niche
EV/exosome-mediated signaling & uptake routes	Engineered EVs/exosome-inspired carriers; homotypic delivery; EV interception	EV-tracking labels; uptake kinetics	Payload delivery via natural internalization; triggerable release	Improves uptake and biocompatibility

## 6. Targeted Delivery-based Treatment: Therapeutic Modalities

Targeted delivery is ultimately validated by therapeutic action at the intended site not only tumor accumulation, but also intratumoral penetration, cellular uptake, and payload activation in the TME. Because tumors present multiple, coupled barriers (limited penetration, hypoxia, redox buffering by GSH, and immunosuppression), single-modality treatment frequently underperforms. Accordingly, many modern nanotherapeutics are designed to co-deliver complementary modalities so that one component removes the bottleneck that limits another.<sup>83</sup>

### 6.1. Chemotherapy delivery

Chemotherapy remains central in cancer care, but its benefit is often constrained by poor tumor accumulation, drug resistance, and systemic toxicity.<sup>84</sup> Nanoparticle drug-delivery systems can address these limitations by extending circulation, improving biodistribution, enabling sustained/controllable release, and reducing systemic toxicity thereby increasing effective drug exposure at tumors.<sup>85</sup>

A key trend is co-delivery of drug pairs that have clinical rationale but suffer from off-target toxicity when administered freely. For example, combined doxorubicin (DOX) and platinum drug regimens are clinically used, yet remain suboptimal due to nonspecific distribution and adverse effects, motivating nanodrug strategies with high loading and tumor-selective activation.<sup>86</sup>

### 6.2. Catalytic ROS-based therapies

Catalytic, ROS-mediated treatment is often integrated with delivery to overcome resistant tumor niches. Chemodynamic therapy (CDT) is defined as a catalyst-dependent process that decomposes endogenous  $H_2O_2$  into cytotoxic hydroxyl radicals ( $\cdot OH$ ) via Fenton or Fenton-like reactions, using catalysts such as  $Mn^{2+}$ ,  $Cu^+$ , or  $Fe^{2+}$ .<sup>87,88</sup> This strategy directly interfaces with the TME, which is frequently characterized by hypoxia, mild acidity, and redox imbalance with high intracellular GSH conditions that can both

enable and suppress catalytic ROS effects.<sup>89</sup>

### 6.3. Light-activated phototherapy

Photothermal and photodynamic strategies are frequently combined with nano-delivery because they enable spatiotemporal control while also amplifying tumor killing through heat and ROS generation. Mn-based nanotherapeutics literature explicitly highlights photodynamic and photothermal approaches as major therapeutic branches, often used in multimodal combinations.<sup>90</sup>

A recurring barrier for photodynamic effects is oxygen limitation in hypoxic tumors. Here,  $MnO_2$ -containing designs are commonly used to convert endogenous  $H_2O_2$  into  $O_2$  and deplete GSH, thereby increasing ROS and improving photodynamic efficiency when coupled with phototherapy.<sup>91</sup> This “oxygenation + redox modulation” logic aligns naturally with targeted delivery: the same tumor-local cues that trigger  $MnO_2$  activity can confine oxygen generation and ROS amplification to tumors, reducing off-target oxidative stress.

### 6.4. Ultrasound-activated nanotherapeutics

Ultrasound (US) provides an attractive external trigger due to its noninvasive and non-ionizing nature, cost efficiency, and ability to focus energy within deep tissues by controlling frequency and focusing parameters.<sup>14</sup> Sonodynamic therapy (SDT) leverages US-activated “sonosensitizers” (often nanoparticle-based) to generate therapeutic effects that can include thermal, mechanical, and sonochemical components not available to purely light-driven methods.<sup>92</sup> Mechanistically, US can enhance local delivery through mechanical effects, while cavitation can drive sonochemical reactions that produce radicals such as  $\cdot OH$  and  $\cdot H$  and subsequently  $H_2O_2$  forming a chemical basis for SDT-mediated ROS generation.<sup>93</sup>

Because SDT is trigger-based, it is naturally compatible with image-guided targeted delivery. Recent SDT nanoparticle systems combine US with imaging readouts to improve treatment accuracy and minimize off-target damage, and emerging examples integrate US with photoacoustic or MR/CT-visible

nanomaterials to track nanoparticle distribution before and during treatment.<sup>94</sup> Notably, exosome-delivered SDT agents have been reported, where tumor-derived exosomes encapsulate a sonosensitizer with therapeutic/imaging capability and enable US-responsive controlled release, enhancing SDT efficacy and tumor specificity in homotypic models.<sup>95</sup>

### 6.5. Immunotherapy integration

A key advantage of nanotherapeutics is their ability to engineer immune activation as part of the delivery payload, rather than treating immunotherapy as a separate drug class administered independently. In Mn-based nanotherapeutics for breast cancer, immunotherapy is framed around activation of innate and adaptive immunity and induction of immunogenic cell death (ICD), with explicit emphasis on the cyclic GMP-AMP synthase (cGAS)-STING pathway and combination with immune checkpoint inhibition.<sup>96</sup>

Mechanistically, several Mn-enabled designs couple ROS generation  $\rightarrow$  ICD  $\rightarrow$  cGAS-STING activation, yielding enhanced antigen presentation and T-cell infiltration. For example, systems are described where TME-responsive Mn release and DOX action generate ROS and ICD, which in turn triggers cGAS-STING signaling.<sup>97</sup> In addition, Mn-nanotherapeutics are frequently positioned as synergistic partners to immune checkpoint inhibitors to amplify overall antitumor immune responses.<sup>98</sup>

## 7. Conclusions

Targeted delivery has become a central design principle in cancer nanotherapeutics because it links where a nanopatform localizes, when it activates, and how it produces measurable therapeutic benefit across the full delivery cascade from circulation stability and tumor access to penetration, cellular uptake, and intracellular trafficking despite inherently conflicting physicochemical requirements at each step. In this review, we highlight how multistage and stimuli-responsive designs resolve these trade-offs through programmable transitions in size, surface charge, and ligand availability, enabling “stealth in

blood” yet “active in tumor” behavior, and we frame the TME as both a transport barrier and an exploitable trigger space where extracellular matrix constraints, hypoxia/acidosis, vascular abnormalities, and immune regulation jointly shape delivery outcomes. We further emphasize delivery-enabled theranostics, in which imaging serves as a functional readout of localization, activation, and response dynamics to guide externally triggered interventions and treatment timing, and we integrate major therapeutic modalities into a delivery-guided combination logic that couples chemotherapy delivery with catalytic reactive oxygen species-based therapies, energy-activated phototherapy or ultrasound-enabled approaches, and immune engagement to exploit TME vulnerabilities while limiting off-target toxicity. Collectively, these concepts position nanotherapeutics not merely as carriers but as coordinated systems that integrate transport, activation, monitoring, and multimodal therapy within tumors, providing a coherent blueprint for targeted delivery-based diagnosis and treatment of cancers.

## Acknowledgements

This study was supported by research fund from Chosun University, 2025.

## Declaration of Competing Interest

The authors declare that there is no conflict of interest.

## References

1. B. K. Kashyap, V. V. Singh, M. K. Solanki, A. Kumar, J. Ruokolainen, and K. K. Kesari, *ACS Omega*, **8**(16), 14290–14320 (2023). <https://doi.org/10.1021/acsomega.2c07840>
2. D. Fan, Y. Cao, M. Cao, Y. Wang, and Y. Cao, T. Gong, *Signal. Transduct. Target. Ther.*, **8**(1), 293 (2023). <https://doi.org/10.1038/s41392-023-01536-y>
3. M. J. Nirmala, U. Kizhuvettil, A. Johnson, B. G. R. Nagarajan, and V. Muthuvijayan, *RSC Adv.*, **13**(13), 8606–8629 (2023). <https://doi.org/10.1039/d2ra07863e>
4. X. Xu, B. Li, K. Xu, and T. Zhang, *Drug. Deliv.*, **33**(1),

- 2605387 (2026). <https://doi.org/10.1080/10717544.2025.2605387>
5. M. A. Phillips, M. L. Gran, and N. A. Peppas, *Nano. Today*, **5**(2), 143-159 (2010). <https://doi.org/10.1016/j.nantod.2010.03.003>
6. J. Wu, *J. Pers. Med.*, **11**(8), (2021). <https://doi.org/10.3390/jpm11080771>
7. U. Prabhakar, H. Maeda, R. K. Jain, E. M. Sevic-Muraca, W. Zamboni, O. C. Farokhzad, S. T. Barry, A. Gabizon, P. Grodzinski, and D. C. Blakey, *Cancer Res.*, **73**(8), 2412-2417 (2013). <https://doi.org/10.1158/0008-5472.CAN-12-4561>
8. C. Ding, C. Chen, X. Zeng, and H. Chen, Y. Zhao, *ACS Nano*, **16**(9), 13513-13553 (2022). <https://doi.org/10.1021/acsnano.2c05379>
9. S. Thakkar, D. Sharma, K. Kalia, and R. K. Tekade, *Acta Biomater.*, **101**, 43-68 (2020). <https://doi.org/10.1016/j.actbio.2019.09.009>
10. U. Hani, V. T. Choudhary, M. Ghazwani, Y. Alghazwani, R. A. M. Osmari, G. S. Kulkarni, H. G. Shivakumar, S. U. D. Wani, and S. Paranthaman, *Pharmaceutics*, **16**(12), (2024). <https://doi.org/10.3390/pharmaceutics16121527>
11. D. C. Joshi, S. Prasad, V. Bhati, P. K. Sharma, N. Joshi, S. Durgapal, M. B. Chavan, V. K. Maurya, V. Subramaniyan, K. R. Paudel, and M. Gupta, *Colloids Surf. B Biointerfaces.*, **258**, 115204 (2026). <https://doi.org/10.1016/j.colsurfb.2025.115204>
12. M. Sharifi, W. C. Cho, A. Ansariesfahani, R. Tarharoudi, H. Malekisarvar, S. Sari, S. H. Bloukh, Z. Edis, M. Amin, J. P. Gleghorn, T. Hagen, and M. Falahati, *Cancers (Basel)*, **14**(12), (2022). <https://doi.org/10.3390/cancers14122868>
13. H. F. Wang, R. Ran, Y. Liu, Y. Hui, B. Zeng, D. Chen, D. A. Weitz, and C. X. Zhao, *ACS Nano*, **12**(11), 11600-11609 (2018). <https://doi.org/10.1021/acsnano.8b06846>
14. Y. Ayyami, M. Dastgir, M. Yektamanesh, H. Zamani, S. S. Jazzi, B. Arjmand, A. P. Siegel, O. A. Mehrizi, R. Manwar, H. Hamishehkar, and K. Avanaiki, *Ultrason Sonochem.*, **127**, 107750 (2026). <https://doi.org/10.1016/j.ultsonch.2026.107750>
15. M. Ikeda-Imafuku, L. L.-W. Wang, D. Rodrigues, S. Shaha, Z. Zhao, and S. Mitragotri, *Journal of Controlled Release.*, **345**, 512-536 (2022). <https://doi.org/10.1016/j.jconrel.2022.03.043>
16. Y. Zhang and J. He, *Acta Biomater.*, **134**, 1-12 (2021). <https://doi.org/10.1016/j.actbio.2021.07.015>
17. S. B. Keller and M. A. Averkiou, *Bioconjug Chem.*, **33**(6), 1049-1056 (2022). <https://doi.org/10.1021/acs.bioconjchem.1c00422>
18. Z. Li, X. Shan, Z. Chen, N. Gao, W. Zeng, X. Zeng, and L. Mei, *Adv. Sci. (Weinh.)*, **8**(1), 2002589 (2020). <https://doi.org/10.1002/advs.202002589>
19. X. Cong, Z. Zhang, H. Li, Y. G. Yang, Y. Zhang, and T. Sun, *J. Nanobiotechnology*, **22**(1), 620 (2024). <https://doi.org/10.1186/s12951-024-02892-9>
20. H. Javid, M. A. Oryani, N. Rezagholinejad, A. Esparham, M. Tajaldini, and M. Karimi-Shahri, *Cancer Med.*, **13**(2), e6800 (2024). <https://doi.org/10.1002/cam4.6800>
21. D. E. Uti, W. A. Omang, E. U. Alum, I. Bawa, O. P. Ugwu, A. O. Idowu, I. J. Atangwho, and G. E. Egbung, *Cancer Med.*, **15**(1), e71519 (2026). <https://doi.org/10.1002/cam4.71519>
22. N. Meher, H. F. VanBrocklin, D. M. Wilson, and R. R. Flavell, *Pharmaceuticals (Basel)*, **16**(2), (2023). 10.3390/ph16020315
23. F. Wang, Z. Li, X. Feng, D. Yang, and M. Lin, *Prostate Cancer and Prostatic Diseases*, **25**(1), 11-26 (2022). <https://doi.org/10.1038/s41391-021-00421-5>
24. D. Makharadze, L. J. Del Valle, R. Katsarava, and J. Puiggali, *Int. J. Mol. Sci.*, **26**(7), (2025). <https://doi.org/10.3390/ijms26073102>
25. I. B. Belyaev, O. Y. Griaznova, A. V. Yaremenko, S. M. Deyev, and I. V. Zelepukin, *Adv. Drug. Deliv. Rev.*, **219**, 115550 (2025). <https://doi.org/10.1016/j.addr.2025.115550>
26. Y. Wang, V. Ukwattage, Y. Xiong, and G. K. Such, *Materials Horizons*, **12**(11), 3622-3632 (2025). <https://doi.org/10.1039/D4MH01781A>
27. V. C. Vetter, M. Yazdi, I. Gialdini, J. Pohmerer, J. Seidl, M. Hohn, D. C. Lamb, and E. Wagner, *Biochemistry*, **64**(7), 1509-1529 (2025). <https://doi.org/10.1021/acs.biochem.4c00650>
28. Y. Hong, W. Ma, M. Wang, and H. H. Wang, *RSC Chem. Biol.*, **6**(9), 1366-1385 (2025). <https://doi.org/10.1039/d5cb00057b>
29. T. Zhang, J. Li, J. Lu, J. Li, H. Zhang, Y. Miao, X. Liu, Y. He, L. Yang, and H. Fan, *Biomaterials*, **315**, 122925 (2025). <https://doi.org/10.1016/j.biomaterials.2024.122925>
30. R. G. A. Mohamed, S. M. Ali, I. S. Ahmed, and M. Rawas-Qalaji, *Z. Hussain, Biomater Sci.*, **13**(20), 5626-

- 5664 (2025). <https://doi.org/10.1039/d5bm01176k>
31. Y. Zhang, Y. Lu, S. Li, F. Zheng, Y. Dong, H. Tang, X. Wang, and J. Wang, *Mater. Today Bio.*, **35**, 102392 (2025). <https://doi.org/10.1016/j.mtbio.2025.102392>
32. F. Veider, E. Sanchez Armengol, and A. Bernkop-Schnürch, *Small*, **20**(3), 2304713 (2024). <https://doi.org/10.1002/sml.202304713>
33. M. Z. Anwar, H. Kathuria, J. X. Er, Y. Wang, and G. N. C. Chiu, *J. Control Release*, **392**, 114719 (2026). <https://doi.org/10.1016/j.jconrel.2026.114719>
34. M. Khan, R. Ullah, G. Wang, and M. Chu, *Theranostics*, **15**(10), 4823-4847 (2025). <https://doi.org/10.7150/thno.108875>
35. H. I. Kim, J. Park, Y. Zhu, X. Wang, Y. Han, and D. Zhang, *Exp. Mol. Med.*, **56**(4), 836-849 (2024). [10.1038/s12276-024-01201-6](https://doi.org/10.1038/s12276-024-01201-6)
36. K. Öztürk, M. Kaplan, and S. Çalıř, *International Journal of Pharmaceutics*, **666**, 124799 (2024). <https://doi.org/10.1016/j.ijpharm.2024.124799>
37. D. C. Joshi, S. Prasad, V. Bhati, P. K. Sharma, N. Joshi, S. Durgapal, M. B. Chavan, V. K. Maurya, V. Subramaniyan, and K. R. Paudel, *Colloids and Surfaces B: Biointerfaces*, **115204** (2025). <https://doi.org/10.1016/j.colsurfb.2025.115204>
38. J. Liu, J. Zhang, Y. Gao, Y. Jiang, Z. Guan, Y. Xie, J. Hu, and J. Chen, *Cancer Letters*, **562**, 216166 (2023). <https://doi.org/10.1016/j.canlet.2023.216166>
39. P. Garidel, A. Blume, and M. Wagner, *Pharmaceutical Development and Technology*, **20**(3), 367-374 (2015). <https://doi.org/10.3109/10837450.2013.871032>
40. J.-Q. Luo, Y.-C. Huang, J.-Y. Zhang, Q.-S. Tong, A. Batool, Y. Duan, and J.-Z. Du, *Biomaterials Science*, **13**(10), 2794-2805 (2025). <https://doi.org/10.1039/D5BM00243E>
41. X. Hu, J. Wu, Y. Chang, M. Zhou, L. Wang, Z. Chen, and Y. Wu, *ACS Applied Nano. Materials*, **9**(8), 3813-3825 (2026). <https://doi.org/10.1021/acsanm.5c05554>
42. S. S. Mashele, *Pharmaceutics*, **17**(8), (2025). [10.3390/pharmaceutics17081082](https://doi.org/10.3390/pharmaceutics17081082)
43. L. Lambuk, M. Z. Sadikan, M. A. Mohd Lazaldin, F. Lambuk, R. Kadir, N. Ismail, and R. Mohamud, *Discov Oncol.*, **17**(1), (2026). <https://doi.org/10.1007/s12672-025-04169-5>
44. W. Wu, L. Luo, Y. Wang, Q. Wu, H. B. Dai, J. S. Li, C. Durkan, N. Wang, and G. X. Wang, *Theranostics*, **8**(11), 3038-3058 (2018). <https://doi.org/10.7150/thno.23459>
45. J. Tao, W. Ning, W. Lu, R. Wang, H. Zhou, H. Zhang, J. Xu, S. Wang, Z. Teng, and L. Wang, *Journal of Controlled Release*, **380**, 85-107 (2025). <https://doi.org/10.1016/j.jconrel.2025.01.058>
46. L. Meng, Y. Zheng, H. Liu, and D. Fan, *Oncologie*, **26**(1), 41-58 (2024). <https://doi.org/10.1515/oncologie-2023-0459>
47. J. Huang, L. Zhang, D. Wan, L. Zhou, S. Zheng, S. Lin, and Y. Qiao, *Signal Transduct Target Ther.*, **6**(1), 153 (2021). <https://doi.org/10.1038/s41392-021-00544-0>
48. X. He, Y. Yang, L. Li, P. Zhang, H. Guo, N. Liu, X. Yang, and F. Xu, *Drug Discovery Today*, **25**(9), 1727-1734 (2020). <https://doi.org/10.1016/j.drudis.2020.06.029>
49. P. Gong, F. Wang, Y. Hua, J. Ying, J. Chen, and Y. Qiao, *J Nanobiotechnology*, **23**(1), 733 (2025). <https://doi.org/10.1186/s12951-025-03815-y>
50. Y. Pi, K. Ganabady, and A. D. Celiz, *Communications Materials*, **6**(1), (2025). <https://doi.org/10.1038/s43246-025-00983-0>
51. D. Averill-Bates, *Biochimica et Biophysica Acta (BBA) - Molecular Cell Research*, **1871**(2), (2024). <https://doi.org/10.1016/j.bbamcr.2023.119573>
52. A. Alhussan, L. Ho, Y. Zhang, H. Fan, A. Momeni, C. Brimacombe, and P. R. Cullis, *J Nanobiotechnology*, **23**(1), 641 (2025). <https://doi.org/10.1186/s12951-025-03704-4>
53. Z. Chen, F. Han, Y. Du, H. Shi, and W. Zhou, *Signal Transduct Target Ther.*, **8**(1), 70 (2023). <https://doi.org/10.1038/s41392-023-01332-8>
54. M. Z. Bakleh and A. Al Haj Zen, *Cells*, **14**(9), (2025). <https://doi.org/10.3390/cells14090673>
55. E. Andreucci, B. S. Fioretto, I. Rosa, M. Matucci-Cerinic, A. Biagioni, E. Romano, L. Calorini, and M. Manetti, *Cells*, **12**(6), (2023). <https://doi.org/10.3390/cells12060939>
56. W. Chen, J. Lai, S. Dong, L. Chen, and H. Yang, *Anal Chem.*, **96**(8), 3462-3469 (2024). <https://doi.org/10.1021/acs.analchem.3c05064>
57. T. Thambi, J. H. Park, and D. S. Lee, *Chemical Communications*, **52**(55), 8492-8500 (2016). <https://doi.org/10.1039/C6CC02972H>
58. O. J. Okesanya, U. O. Adebayo, L. A. Habeeb, A. Gilbert, M. F. H. Lamem, M. M. Ahmed, T. A. Oso, and D. E. Lucero-Prisno, *One Health Advances*, **4**(1), (2026). <https://doi.org/10.1016/j.ohadv.2026.100001>

- doi.org/10.1186/s44280-026-00107-4
59. S. Guelfi, K. Hodivala-Dilke, and G. Bergers, *Nature Reviews Cancer*, **24**(10), 655-675 (2024). <https://doi.org/10.1038/s41568-024-00736-0>
  60. M. A. Harris, P. Savas, B. Virassamy, M. M. O'Malley, J. Kay, S. N. Mueller, L. K. Mackay, R. Salgado, and S. Loi, *Nature Reviews Cancer*, **24**(8), 554-577 (2024). <https://doi.org/10.1038/s41568-024-00714-6>
  61. S. L. Li, H. Y. Hou, X. Chu, Y. Y. Zhu, Y. J. Zhang, M. D. Duan, J. Liu, and Y. Liu, *ACS Nano*, **18**(11), 7769-7795 (2024). <https://doi.org/10.1021/acsnano.3c12387>
  62. N. Khatoun, Z. Zhang, C. Zhou, and M. Chu, *Biomaterials Science*, **10**(5), 1193-1208 (2022). <https://doi.org/10.1039/D1BM01164D>
  63. Y. Yao, H. Chen, and N. Tan, *Acta Pharm Sin B*, **12**(4), 2103-2119 (2022). <https://doi.org/10.1016/j.apsb.2021.10.010>
  64. R. Butti, A. Khaladkar, P. Bhardwaj, and G. Prakasam, *Cancer Drug Resist*, **6**(1), 182-204 (2023). <https://doi.org/10.20517/cdr.2022.72>
  65. Z. Mai, Y. Lin, P. Lin, X. Zhao, and L. Cui, *Cell. Death. Dis.*, **15**(5), 307 (2024). <https://doi.org/10.1038/s41419-024-06697-4>
  66. H. Zhang, X. Yue, Z. Chen, C. Liu, W. Wu, N. Zhang, Z. Liu, L. Yang, Q. Jiang, Q. Cheng, P. Luo, and G. Liu, *Mol. Cancer*, **22**(1), 159 (2023). <https://doi.org/10.1186/s12943-023-01860-5>
  67. M. B. Schank, J. Zhao, L. Wang, J. P. Moorman, and Z. Q. Yao, *Biomedicines*, **14**(3), (2026). <https://doi.org/10.3390/biomedicines14030495>
  68. M. S. Kishta, A. Khamis, H. Am, A. H. Elshaar, and D. Gul, *Transl Oncol.*, **51**, 102216 (2025). <https://doi.org/10.1016/j.tranon.2024.102216>
  69. D. R. Serrano, F. Juste, B. J. Anaya, B. I. Ramirez, S. A. Sanchez-Guirales, J. M. Quispillo, E. M. Hernandez, J. A. Simon, J. M. Trallero, C. Serrano, S. Rawat, and A. Lalatsa, *Pharmaceutics*, **17**(10), (2025). <https://doi.org/10.3390/pharmaceutics17101336>
  70. K. K. Lee, K. W. Park, S. C. Lee, and C. S. Lee, *Theranostics*, **15**(3), 1077-1093 (2025). <https://doi.org/10.7150/thno.102743>
  71. M. Khan, R. Ullah, S. M. Shah, U. Farooq, and J. Li, *ACS Applied Bio Materials*, **8**(5), 3571-3600 (2025). <https://doi.org/10.1021/acsbm.5c00040>
  72. D. Özel and F. Yurt, *Inorganic Chemistry Communications*, **179**, 114713 (2025).
  73. C. Geraldes, *Molecules*, **29**(23), (2024). <https://doi.org/10.3390/molecules29235591>
  74. F. Yanar, D. Carugo, and X. Zhang, *Molecules*, **28**(15), (2023). <https://doi.org/10.3390/molecules28155694>
  75. J. Yao, T. Munoz-Ortiz, F. Sanz-Rodriguez, E. Martin Rodriguez, D. H. Ortgies, J. Garcia Sole, D. Jaque, and R. Marin, *ACS Photonics*, **9**(2), 559-566 (2022). <https://doi.org/10.1021/acsp Photonics.1c01504>
  76. Y. Zhang, S. Lei, Y. Pan, C. Zhao, Q. Liu, Y. Wu, Y. Liu, M. Li, P. Huang, and J. Lin, *Chinese Chemical Letters*, 110977 (2025). <https://doi.org/10.1016/j.ccllet.2025.110977>
  77. H. Lu, A. Chen, X. Zhang, Z. Wei, R. Cao, Y. Zhu, J. Lu, Z. Wang, and L. Tian, *Nat Commun.*, **13**(1), 7948 (2022). <https://doi.org/10.1038/s41467-022-35655-x>
  78. J. Song, H. Wang, X. Meng, W. Li, and J. Qi, *Nat Commun.*, **15**(1), 10395 (2024). <https://doi.org/10.1038/s41467-024-53906-x>
  79. W. M. Girma, S. L. Mekuria, G. Gedda, X. Shi, Y.-J. Park, and M.-G. Pang, *Coordination Chemistry Reviews*, **548**, (2026). <https://doi.org/10.1016/j.ccr.2025.217236>
  80. Q. Sun, Q. You, J. Wang, L. Liu, Y. Wang, Y. Song, Y. Cheng, S. Wang, F. Tan, and N. Li, *ACS Appl Mater Interfaces.*, **10**(2), 1963-1975 (2018). <https://doi.org/10.1021/acsami.7b13651>
  81. N. Mhlanga, N. Mphuthi, H. Van der Walt, S. Nyembe, T. Mokhena, and L. Sikhwivhilu, *Materials Today Chemistry*, **40**, 102233 (2024). <https://doi.org/10.1016/j.mtchem.2024.102233>
  82. D. Monsalvez-Romin, N. Martinez-Albert, M. C. Garcia-Domene, and S. Orti-Navarro, *J. Clin Med.*, **14**(24), (2025). <https://doi.org/10.3390/jcm14248795>
  83. K. Benderski, T. Lammers, and A. M. Sofias, *Nat Nanotechnol*, **20**(8), 1163-1172 (2025). <https://doi.org/10.1038/s41565-025-01932-1>
  84. U. Anand, A. Dey, A. K. S. Chandel, R. Sanyal, A. Mishra, D. K. Pandey, V. De Falco, A. Upadhyay, R. Kandimalla, A. Chaudhary, J. K. Dhanjal, S. Dewanjee, J. Vallamkondu, and J. M. Perez de la Lastra, *Genes Dis.*, **10**(4), 1367-1401 (2023). <https://doi.org/10.1016/j.gendis.2022.02.007>
  85. M. Mittal, S. Juneja, N. Pandey, and R. Mittal, *Current Drug Targets*, (2025). <https://doi.org/10.2174/0113894501393535250903071153>
  86. F. D. Kalindemirtas, G. E. Cilasan, and A. Kariper, *Naunyn*

- Schmiedebergs Arch Pharmacol.*, **398**(10), 14367-14383 (2025). <https://doi.org/10.1007/s00210-025-04080-4>
87. K. K. Lee, J. W. Kim, C. S. Lee, and S. C. Lee, *J. Control Release*, **361**, 350-360 (2023). <https://doi.org/10.1016/j.jconrel.2023.07.050>
88. Q. Zhang, Q. Luo, Z. Liu, M. Sun, and X. Dong, *Chemical Engineering Journal*, **457**, (2023). <https://doi.org/10.1016/j.cej.2022.141225>
89. J.-H. Jang, D.-H. Kim, and K.-S. Chun, *Archives of Pharmacal Research*, **48**(2), (2025). <https://doi.org/10.1007/s12272-025-01532-6>
90. S. Wang, Y. Zou, L. Hu, and Y. Lv, *Acta Biomater.*, **191**, 369-385 (2025). <https://doi.org/10.1016/j.actbio.2024.11.010>
91. R. Zhou, X. Zeng, H. Zhao, Q. Chen, and P. Wu, *Coordination Chemistry Reviews*, **452**, 214306 (2022).
92. P. Cressey, S. B. Abd Shukor, and M. Thanou, *Adv Drug Deliv Rev.*, **226**, 115696 (2025). <https://doi.org/10.1016/j.addr.2025.115696>
93. T. Zhang, Y. Jin, R. Yu, Y. Li, and H. Wu, *WFUMB Ultrasound Open*, **4**(1), (2026). <https://doi.org/10.1016/j.wfumbo.2025.100100>
94. M. Pan, D. Hu, L. Yuan, Y. Yu, Y. Li, and Z. Qian, *Acta Pharm Sin. B.*, **13**(7), 2926-2954 (2023). <https://doi.org/10.1016/j.apsb.2022.12.021>
95. G. Chiabotto, M. Conte, and V. Cauda, *Cancers (Basel)*, **18**(1), (2025). <https://doi.org/10.3390/cancers18010118>
96. M. Khan, R. Ullah, S. M. Shah, U. Farooq, and J. Li, *ACS Appl. Bio. Mater.*, **8**(5), 3571-3600 (2025). <https://doi.org/10.1021/acsabm.5c00040>
97. Z. Zhang, J. Yang, Q. Zhou, S. Zhong, J. Luo, X. Chai, J. Liu, X. Zhang, X. Chang, and H. Wang, *Redox Biol.*, **85**, 103761 (2025). <https://doi.org/10.1016/j.redox.2025.103761>
98. C. Xu, F. Wu, Z. Duan, B. Rajbanshi, Y. Qi, J. Qin, L. Dai, C. Liu, T. Jin, B. Zhang, and X. Zhang, *J Nanobiotechnology*, **23**(1), 330 (2025). <https://doi.org/10.1186/s12951-025-03383-1>